RESEARCH ARTICLE

Mechanism of β-sitosterol on phenotype switch of vascular smooth muscle cells induced by angiotensin II

Siqing He[1], Shumiao He[1], Yuankun Chen[1], Xiaobao Jin[2], Wenjie Mei[3], Qun Lu[1, 2, 3, *]

[1]School of Life Sciences and Biopharmaceutics, [2]Guangdong Province Key Laboratory of Pharmaceutical Bioactive Substances, Guangdong Pharmaceutical University, Guangzhou, Guangdong, China. [3]Guangdong Province Engineering and Technology Center for Molecular Probe and Bio-medicine Imaging, Guangzhou, Guangdong, China.

Received: February 23, 2024; **accepted:** May 13, 2024.

The phenotype switch of vascular smooth muscle cells (VCMCs) is involved in the progression of atherosclerosis (AS). β-sterols (BS), a natural product, has been found to be effective in the treatment of AS, but whether it is related to the inhibition of VCMCs phenotype switching remains unknown. Therefore, the aim of this study was to investigate the effect of BS on angiotensin II (Ang II)-induced phenotype switching of VCMCs. The Cell Counting Kit-8 (CCK8) method was used to determine the relative cell viability. Scratch Assay was applied to investigate the rate of cell migration, and western blotting was performed to identify the expression level of the target protein. Actin-Tracker Green was used to observe the changes in cytoskeleton and morphology. The mRNA level of collagen II was analyzed by real-time quantitative polymerase chain reaction (q-PCR). In addition, the network pharmacology was employed to predict the mechanism of BS inhibiting phenotype switch. The results demonstrated that BS might effectively restrain the phenotype switch of VSMCs, and the optimal inhibition occurred when cells were treated with 4 μg/mL BS for 24 h. Moreover, BS were proved to inhibit overproliferation, overmigration, skeletal remodeling, and secretion of VSMCs. The results also suggested that BS might inhibit the phenotype switch of VSMCs through the cAMP/PKA/CREB signaling pathway and inhibit excessive cell proliferation, overmigration, secretion, and skeletal remodeling during this process. This study provided new ideas for finding targets and developing new drugs for cardiovascular diseases such as atherosclerosis.

Keywords: β-sterol; Ang Ⅱ; phenotype switch; network pharmacology; cAMP/PKA/CREB signaling pathway.

[*]**Corresponding author:** Qun Lu, School of Life Sciences and Biopharmaceutics, Guangdong Pharmaceutical University, Guangzhou, Guangdong, China. Phone: +86 13725379776. Email: lugun2@126.com.

Introduction

Cardiovascular diseases affect 26% of the global population and will cause more than 23 million deaths by 2030. Atherosclerosis (AS) is the pathological basis of cardiovascular diseases, which seriously threatens people's health [1-3]. Some studies have shown that AS is related to the phenotype switch of vascular smooth muscle cells (VSMCs) that can maintain the physiological function and structural integrity of the vascular wall under normal conditions. However, under the stimulation of various stimulating factors such as angiotensin II (Ang II), the phenotype switch of VSMCs can occur and accompany by abnormal proliferation and migration of VSMCs

as well as the synthesis of a large number of extracellular matrix, which ultimately leads to the occurrence of proliferative vascular diseases and involve in cardiovascular diseases such as atherosclerosis [4-6]. Therefore, prevention of phenotypic switching of VSMCs may help to alleviate the process of cardiovascular diseases such as AS.

β-sitosterol (BS) exists in various natural plants and does not have cytotoxicity [7]. BS has been reported to have antioxidant, antibacterial, anti-inflammatory, and cholesterol-regulating effects [8-12]. In addition, BS has also been reported in the treatment of cardiovascular diseases. For example, BS may compete with the absorption site of cholesterol, inhibit the absorption of cholesterol in the intestine, reduce the level of cholesterol in the blood, and fight atherosclerosis [13]. BS can also inhibit the excessive proliferation of VCMCs by upregulating the expression of p21cip1 protein [14]. However, currently, there is no report on whether BS exerts its effect by inhibiting phenotype switch of VSMC.

A7r5 cells are often used as research objects to study the mechanisms related to atherosclerosis. Qin *et al*. used A7r5 cells to study the inhibitory effect of recombinant human CXCL8(3-72)K11R/G31P on atherosclerotic plaques [15]. Zhang *et al*. used A7r5 cells to study the effect of *Tribulus terrestris* extract on atherosclerosis [16]. Network pharmacology is an effective approach to study the complex relationship between Chinese herbal medicine and diseases, which can integrate laboratory and clinical investigations with data processing to guide drug discovery and development [17]. Therefore, this study aimed to investigate the relationship between BS and phenotype switch of VSMCs by using A7r5 cells to find and verify the key targets and pathways based on network pharmacology. The results of this study would provide new ideas for the application of new drugs to block the phenotype switch of VSMCs and treat cardiovascular diseases.

Materials and methods

Cell culture and treatment

A7r5 cells were purchased from the Cell Bank of the Chinese Academy of Sciences (Shanghai, China), which can represent the VSMCs. The A7r5 cells were cultured in Dulbecco's Modified Eagle Medium (DMEM) supplemented with 10% fetal bovine serum (FBS) (Thermo Fisher Scientific, Waltham, MA, USA) and 5% CO_2 at 37°C [18]. Cells were divided into 4 groups and were treated respectively with Ang II (Meilunbio, Dalian, China) at 0, 1, 2, 4, 8 μg/mL, β-sitosterol (Meilunbio, Dalian, China) at 0, 1, 2, 4, 8, 16 μg/mL, Ang II (2 μg/mL) and BS (1, 2, 4 μg/mL) with 10 μg/mL telmisartan (Tel) as positive control (Meilunbio, Dalian, China), and Ang II (2 μg/mL) with BS (4 μg/mL) and 12 μM H-89 (Beyotime, Shanghai, China), a protein kinase A (PKA) inhibitor.

Cell counting kit-8 (CCK8) assay

A7r5 cells were inoculated in 96-well plates and 10 μL CCK8 (Beyotime, Shanghai, China) was added to each well. After culturing for 4 hrs, the absorbance was measured at the wavelength of 450 nm using a Bio-Rad M450 microplate reader (Bio-Rad, Hercules, CA, USA) [19]. The cell survival rate was calculated using the following formula.

$$\text{Cell survival rate (\%)} = [(As-Ab)/(Ac-Ab)] \times 100\%$$

where As was the absorbance of the experimental groups. Ab was the absorbance of blank group. Ac was the absorbance of the control group.

Western blotting

The protein sample was obtained by lysing the cells with RIPA buffer (Beyotime, Shanghai, China) and then quantitated with BCA Protein Quantification Kit (Beyotime, Shanghai, China) following the manufacturer's instructions. The Western Blot experiments were done with different primary antibodies including proliferating cell nuclear antigen (PCNA), SM22α, α-SMA, OPN, PKA, phospho-PKA, CREB, phospho-CREB, GAPDH (Abcam, Cambridge, UK) and ECL

kit (Beyotime, Shanghai, China) following the manufacturers' instructions [20]. The images were analyzed using Image J software (Media Cybernetics, Rockville, Maryland, USA).

Cell scratch assay

Cells were inoculated into 6-well plates when the cell density reached 80-90%. After removing original media and washing the cells twice with phosphate buffer solution (PBS), the floating cells were removed, and the photos of cells were taken using an inverted microscope (Sartorius, Göttingen, Germany). The cells' migration situation was observed and photographed after 24 h incubation. Each concentration was tested with three repeats and nine image fields were shot in each well [21]. The distances of scratches on images were measured using Image J software. The scratch distance of each visual field was defined as the mean value of the distances of the three scratch edges in the visual field.

Actin-tracker green staining

5×10^5 cells were collected and seeded in 12-well plates and treated with different drugs when the cell density reached 80-90% for different cell groups. After 24 h of incubation, the cells were washed twice with PBS, fixed with poly-formaldehyde for approximately 15 mins, incubated with 200 µL diluted Actin-Tracker Green (Beyotime, Shanghai, China) per well for 60 mins, re-stained with DAPI (Beyotime, Shanghai, China) for 5 mins, and then added anti-fluorescence quencher (Beyotime, Shanghai, China). The images were acquired using a fluorescence microscopy (Olympus, Tokyo, Japan) at 40× magnification [22].

Real-time quantitative polymerase chain reaction (qPCR)

The total RNAs of the cells were extracted using Trizol method and quantified using an ultramicro spectrophotometer (Thermo Fisher Scientific, Waltham, MA, USA). The reverse transcription reaction was then carried out using 4× Reverse Transcription master mix (EZBioscience, Roseville, MN, USA) at 42℃ for 15 mins followed by 95℃ for 30 s following manufacturer's instructions. The primers for Collagen I gene were 5'-TGC AAG AAC AGC GTA GCC-3' (forward) and 5'-GAG CCA TCC ACA AGC GT-3' (reverse), while the primers for GAPDH gene were 5'-CAA CGT GTC AGT GGT GGA CCT G-3' (forward) and 5'-GAG CCA TCC ACA AGC GT-3' (reverse). All primers were synthesized by Sangong BioEngineering Co., LTD. (Shanghai, China). The qPCR was performed using 2× SYBR Green qPCR master mix (EZBioscience, Roseville, MN, USA) following the manufacturer's instructions. The CFX Connect Real-Time PCR Detection System (Bio-Rad Laboratories, Hercules, CA, USA) was employed for qPCR reaction with the program of 95°C for 5 mins followed by 40 cycles of 95°C for 10 s and 60°C for 30 s.

The enzyme-linked immunosorbent assay (ELISA)

The cells were inoculated into 96-well plates and treated with different concentrations of drugs for 24 h. The content of cAMP in the supernatant of cultured cells was determined using the ELISA Kit (ElabScience, Wuhan, Hubei, China) following manufacturer's instructions.

Prediction of mechanism based on network pharmacology

The possible targets of BS were obtained from the Traditional Chinese Medicine Systems Pharmacology Database and Analysis Platform (TCMSP) (https://tcmsp-e.com/tcmsp.php) or by importing the two-dimensional structure of BS from DrugBank (https://go.drugbank.com) into Pharmmapper (http://www.lilab-ecust.cn/pharmmapper) and Swiss Target Prediction databases (http://www.swisstargetprediction.ch). The targets related to phenotype switch were obtained from the Gene Card database (https://www.genecards.org). All the targets were imported into Veen for online mapping (https://bioinfogp.cnb.csic.es/tools/venny). The common targets were identified and analyzed using STRING (https://cn.string-db.org) and Cytoscape_v3.8.2 (https://cytoscape.org) to obtain the core targets. KEGG (https://www.genome.jp/kegg) and GO

(https://www.geneontology.org) analyses were then conducted using the David database (https://david.ncifcrf.gov) to predict possible signaling pathways [23]. The three-dimensional structures of BS and pathway protein were obtained from the RCSB Protein Data Bank (www.rcsb.org), and then dehydrogenated and hydrated using Discovery Studio 4.0 (https://www.3dsbiovia.com) and docked with AutoDockTools-1.5.6 (https://autodocksuite.scripps.edu).

Statistical analysis

GraphPad Prism7 (GraphPad, San Diego, CA, USA) was employed for data processing and analysis of this study. One-way analysis of variance (ANOVA) was used to identify the differences of data among the multiple samples. *P* value less than 0.05 was set as significant difference, while *P* value less than 0.01 as very significant difference.

Results

β-Sitosterol inhibited the excessive proliferation of VSMCs

To screen the appropriate Ang II concentration, CCK-8 was used to detect cell activities. The results showed that, after incubating cells with 0, 1, 2, 4, 8 μg/mL Ang II for 6, 12, 24, and 48 h, the 2 μg/mL Ang II treated cells demonstrated higher cell activities than that of other Ang II concentrations, especially for 24 h incubation ($P < 0.05$). Therefore, 2 μg/mL Ang II for 24 h treatment was selected for all the other experiments (Figure 1a). The cells were then treated with 0, 1, 2, 4, 8, 16 μg/mL BS for 6, 12, 24, and 48 h to determine the effect of BS on cell activity. The results showed that the cell activity decreased significantly when BS concentrations were 8 and 16 μg/mL ($P < 0.05$) (Figure 1b). Therefore, the BS concentrations of 1, 2, and 4 μg/mL were determined as the experimental conditions. Then CCK-8 was used to detect the effect of BS on the proliferation of ANGII-induced VSMCs. The results showed that Ang II induced the proliferation of VSMCs compared with the control group, while the addition of BS inhibited the proliferation activity of the cells ($P < 0.05$) (Figure 1c). The expression level of PCNA was up-regulated by Ang II and down-regulated by BS treatment compared with the control group ($P < 0.05$) (Figure 1d).

β-Sitosterol inhibited the phenotype switch of VSMCs

The effect of BS on the phenotype switch of cells induced by Ang II was investigated using western blotting to determine the expression levels of cell phenotype switch-related proteins including SM22α, α-SMA, and OPN. The results showed that Ang II significantly down-regulated the expression of SM22α and α-SMA and up-regulated the expression of OPN compared with that in the control group, while BS treatment reversed the effect of Ang II ($P < 0.05$) (Figure 2).

β-Sitosterol inhibited overmigration, skeleton remodeling and reduced secretion of VSMCs

The scratch assay demonstrated that Ang II induced cell migration, while BS treatment slowed Ang II-induced migration compared with the control group ($P < 0.05$) (Figure 3a). Actin-tracker green staining results showed that the cell morphology was fusiform, containing a small number of microfilaments, and the cytoskeletal F-actin was mostly distributed in a punctate pattern in control group. After Ang II treatment, the number of microfilaments increased, and the cytoskeletal F-actin was mostly distributed in filamentous patterns. However, this change was reversed by the addition of BS (Figure 3b). The qPCR results showed that Ang II enhanced the mRNA level of collagen I compared with that in the control group, while BS reversed the enhanced effect of Ang II ($P < 0.05$) (Figure 3c).

Prediction by network pharmacology

A total of 71 common targets were obtained for BS and phenotype switch (Figure 4a). By importing these targets into STRING and visualizing them using Cyto-scape, it was found that BS might regulate VCMCs phenotype switch through multiple targets such as JUN, APP, NR3C1, CASP3, GSK3B, *etc*. (Figure 4b). The results of GO functional annotation suggested

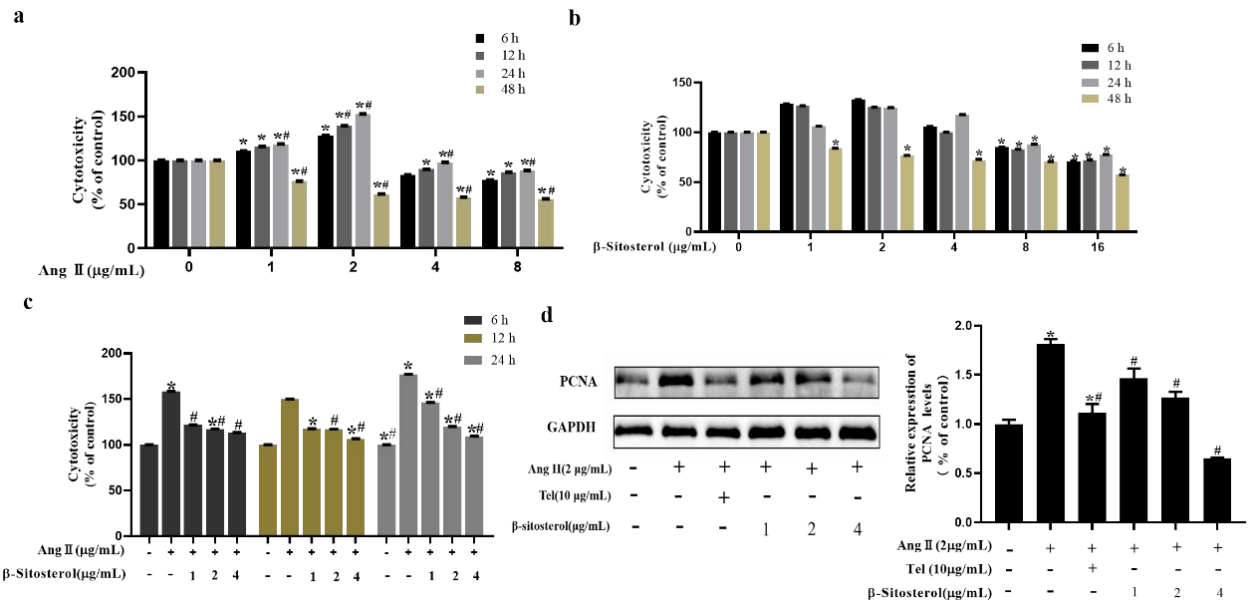

Figure 1. BS inhibited Ang II-induced excessive proliferation of VSMCs. **a.** The effect of various concentrations of Ang II on VSMCs viability. **b.** The effect of BS on VSMCs activity. **c.** The effect of BS on Ang II-induced VSMCs proliferation. **d.** Western Blot imaging and density analysis histogram of PCNA. **#:** $P < 0.05$ compared to control group. ***:** $P < 0.05$ compared to Ang II group.

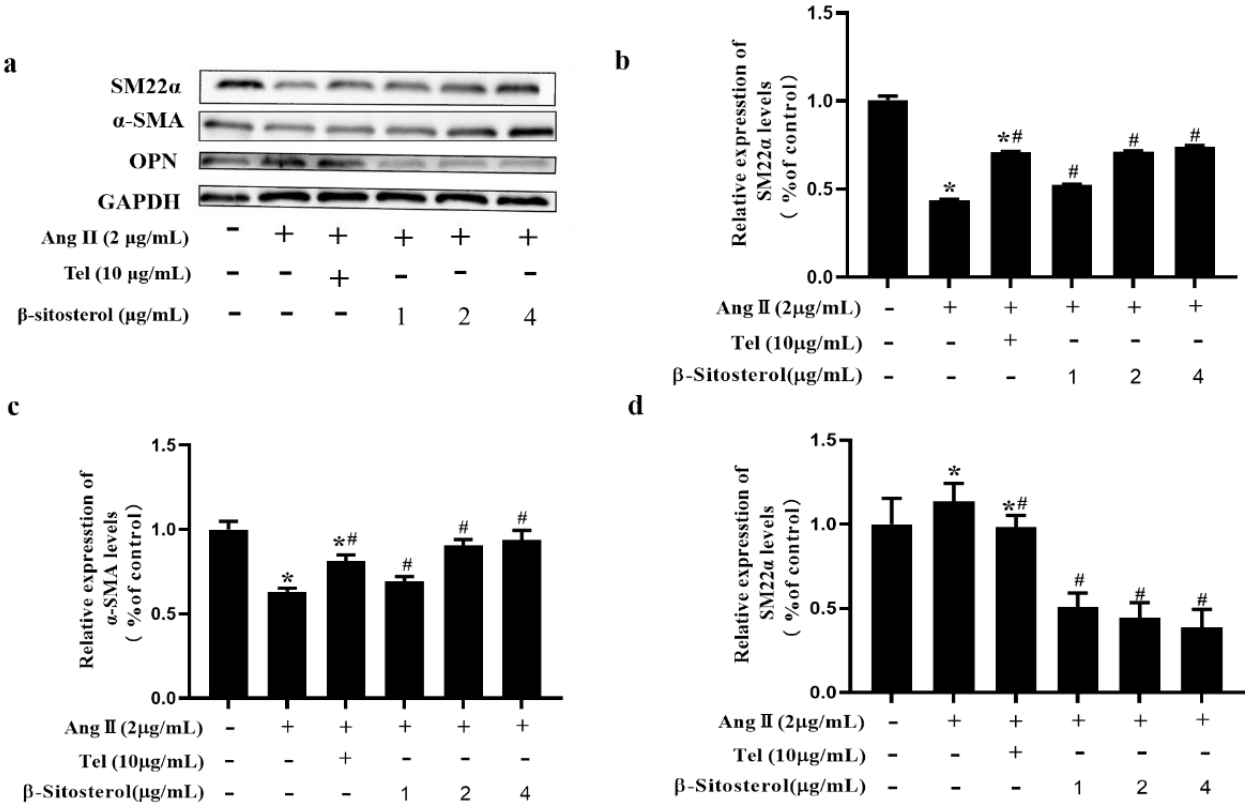

Figure 2. BS inhibited phenotype switch of VSMCs. **a.** Western Blot imaging of SM22α, α-SMA, and OPN. **b.** The density analysis histogram of SM22α. **c.** The density analysis histogram of α-SMA. **d.** The density analysis histogram of OPN. **#:** $P < 0.05$ compared to control group. ***:** $P < 0.05$ compared to Ang II group.

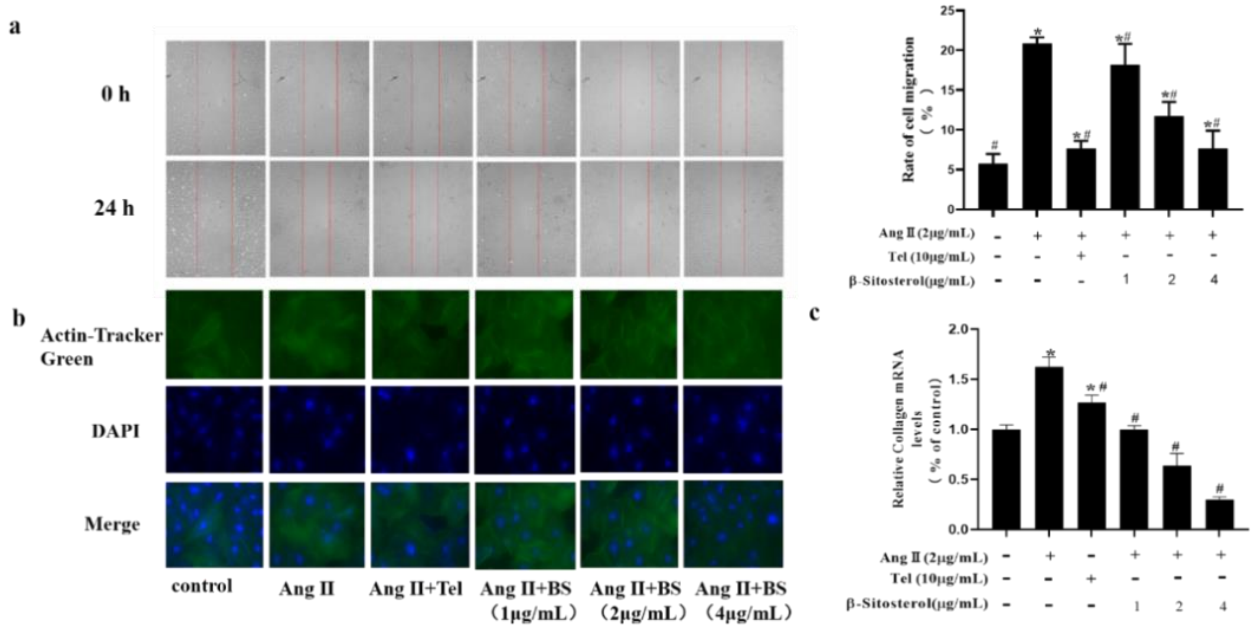

Figure 3. BS inhibited overmigration, skeleton remodeling, and reduced secretion of VSMCs. **a.** Cell scratch morphology diagram and histogram of cell migration rate. **b.** Actin-Tracker Green staining photograph. **c.** Collagen I mRNA expression levels. **#:** $P < 0.05$ compared to control group. ***:** $P < 0.05$ compared to Ang II group.

that some biological processes were mainly involved including positive regulation of the MAPK cascade, positive regulation of ERK1, and some molecular functions including enzyme binding and acting on some cellular components such as integral components of the presynaptic membrane (Figure 4c). KEGG pathway analysis found that BS mainly participated in calcium, cAMP, and other signaling pathways (Figure 4d). According to the previous studies [24, 25], cAMP signaling pathway was selected for furth investigation. Molecular docking results demonstrated that BS bound well to cAMP, PKA, and cAMP response element-binding protein (CREB), which all are important proteins in cAMP signaling pathway with binding energies of -7.0, -9.7, and -9.4 kj/mol, respectively (Figure 4e).

β-Sitosterol inhibited phenotype switch of VSMCs *via* cAMP/PKA/CREB signaling pathway

Western blotting results showed that the ratios of p-PKA/PKA and p-CREB/CREB were decreased in the Ang II treatment group compared with that in the control group, while the ratios of p-PKA/PKA and p-CREB/CREB were increased after BS treatment ($P < 0.05$) (Figure 5a-c). In addition, ELASA results showed that BS reversed the decrease in cAMP concentration in Ang II treatment cells compared to that in the control group ($P < 0.05$) (Figure 5d). For further verification, the cells were treated with PKA inhibitor, H-89, in addition to BS. The results showed that H-89 blocked the upregulation of SM22α and α-SMA expression and upregulated OPN expression compared with that in BS group ($P < 0.05$) (Figure 5e-h), which suggested that BS inhibited Ang II-induced phenotypic switching in A7r5 cells through the cAMP/PKA/CREB signaling pathway.

β-Sitosterol inhibited excessive proliferation, overmigration, skeleton remodeling, and secretion of VSMCs *via* cAMP/PKA/CREB signaling pathway

After treating cells with H-89, the expression of PCNA and cell survival rate increased compared with that in Ang II + BS group (Figure 6a-c), while the migration rate of A7r5 cells was also accelerated (Figure 6d). Most of the skeleton F-actin distribution was filamentous (Figure 6e), and the mRNA expression levels of Collagen I were also increased (Figure 6f). The results

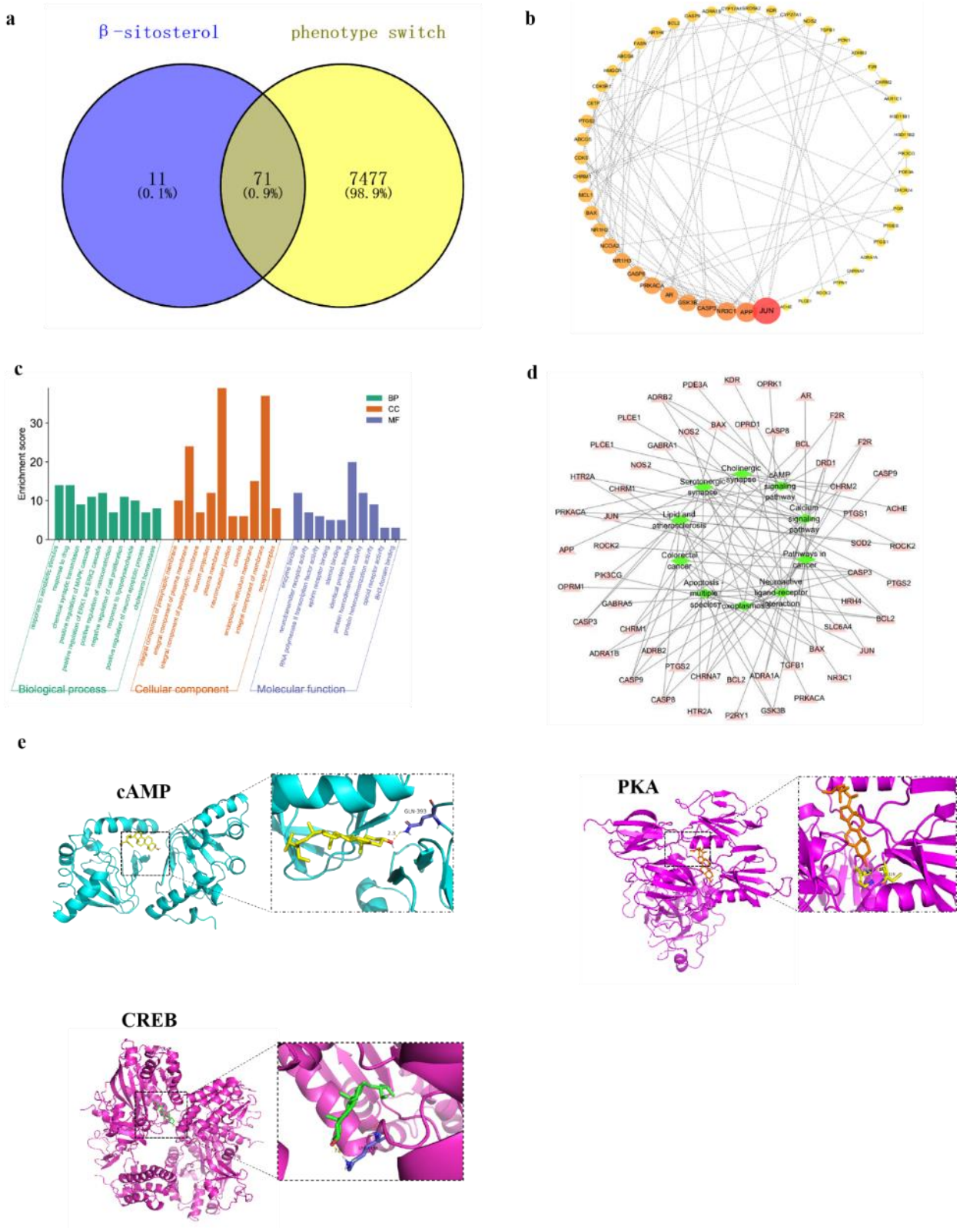

Figure 4. Prediction by network pharmacology. **a.** Veen diagram of the common targets of BS and phenotype switch. **b.** Visual analysis of common target protein interaction network. **c.** GO enrichment analysis. **d.** Mapping of BS-phenotypic switch targets and pathways. **e.** Molecular docking of BS with cAMP, PKA, and CREB.

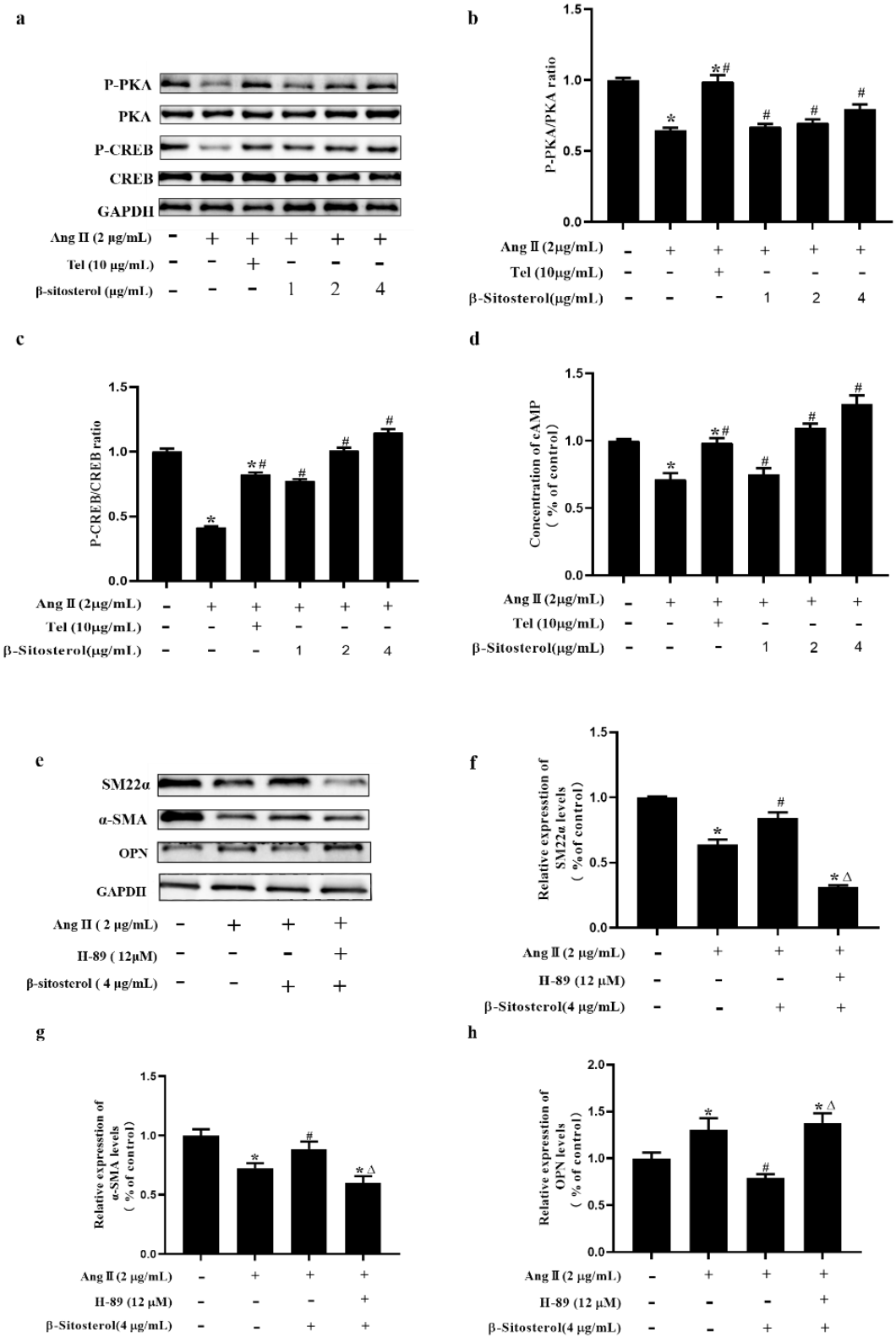

Figure 5. BS inhibited phenotype switch of VSMCs *via* cAMP/PKA/CREB signaling pathway. **a.** Western Blot imaging of PKA and CREB. **b.** The density analysis histogram of P-PKA/PKA. **c.** The density analysis histogram of P-CREB/CREB. **d.** The relative level analysis histogram of cAMP. **e.** Western Blot imaging of SM22α, α-SMA, and OPN. **f.** The density analysis histogram of SM22α. **g.** The density analysis histogram of α-SMA. **h.** The density analysis histogram of OPN. **#:** $P < 0.05$ compared to control group. ***:** $P < 0.05$ compared to Ang II group. **Δ:** $P < 0.05$ compared to Ang II + BS group.

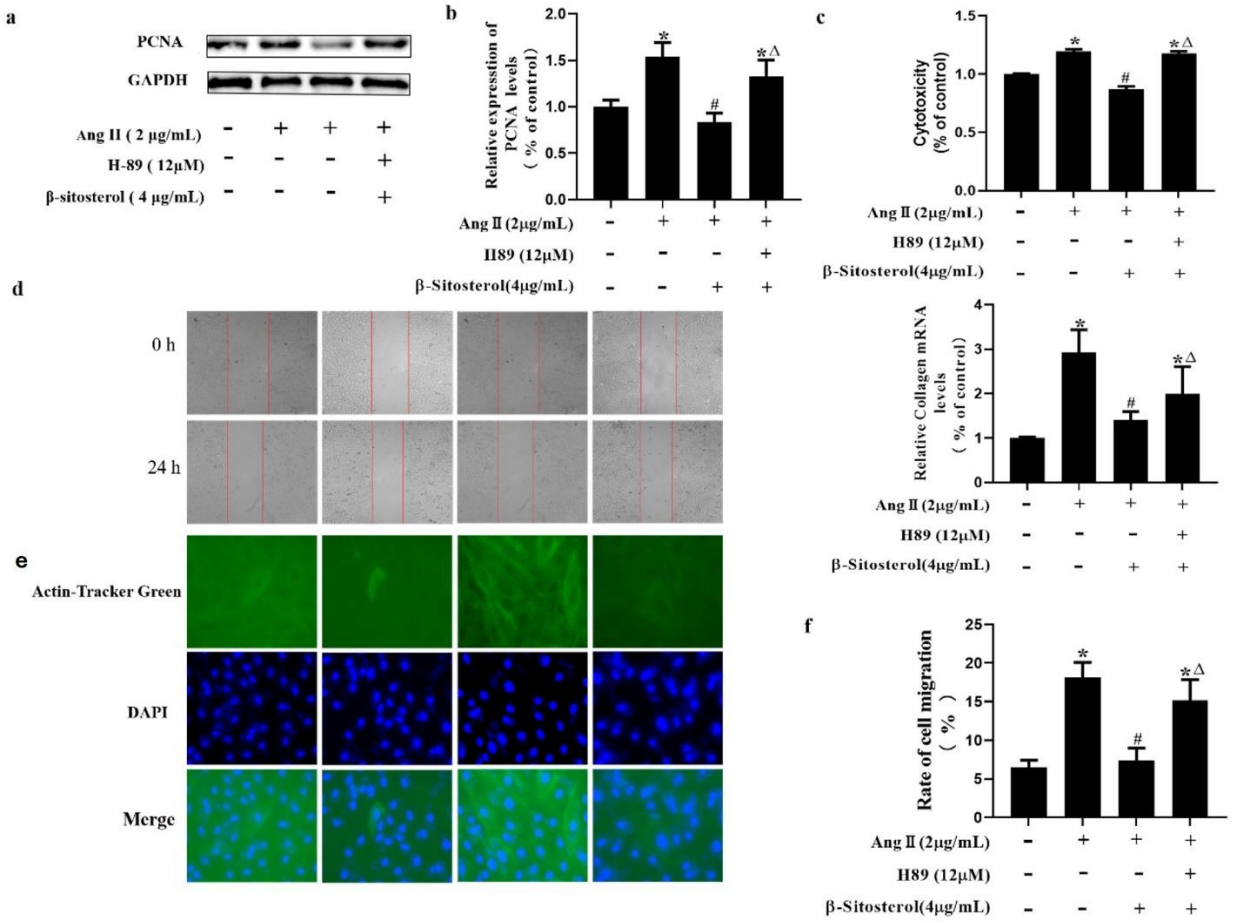

Figure 6. BS inhibited excessive proliferation, overmigration, skeleton remodeling, and secretion of VSMCs *via* cAMP/PKA/CREB signaling pathway. **a.** Western Blot imaging of PCNA. **b.** PCNA density analysis histogram. **c.** A7r5 cell proliferation was detected by CCK8. **d.** Cell scratch morphology diagram and Histogram of cell migration rate. **e.** Actin-Tracker Green staining photograph. **f.** mRNA level of Collagen I. **#:** $P < 0.05$ compared to control group. ***:** $P < 0.05$ compared to Ang II group. **△:** $P < 0.05$ compared to Ang II + BS group.

suggested that BS inhibited the excessive proliferation, overmigration, skeletal remodeling, and secretion of VSMCs *via* the cAMP/PKA/CREB signaling pathway.

Discussion

Phenotype switch of VSMCs was involved in a variety of cardiovascular diseases such as atherosclerosis, aneurysm, restenosis after stenting, *etc*. [26-28]. The research on the mechanism of phenotype switch of VSMCs is helpful to the treatment of cardiovascular diseases. BS has been reported to have an anti-atherosclerotic effect, and atherosclerosis is related to the phenotype switch of VSMCs. Therefore, this study aimed to explore the relationship between BS and phenotype switch using A7r5 cells that have been used as model cells in many cardiovascular studies because they retain many features of VSMCs [29-31]. Ang II is a classic inducer of phenotype switch of VSMCs [32-35]. The phenotype switch of VSMCs is associated with excessive proliferation [36, 37]. The expression level of PCNA is an important index for evaluating cell proliferation [38-41], which can improve the stability of DNA replication, regulate cell growth, and maintain cell's basic functions [42]. This study found that BS could down-regulate PCNA expression in Ang II-induced VSMCs, indicating that BS could inhibit

the proliferation of VSMCs induced by Ang II. SM22α inhibits phenotype switch of VSMCs and plaque formation during atherosclerosis [43]. α-SMA is also abundantly expressed in contractile smooth muscle cells [44]. In addition, phenotype switch can lead to excessive deposition of collagen, which is related to OPN [45]. The expression levels of SM22α and α-SMA decrease when phenotype switch occurs, while the expression level of OPN increases. The results of this study showed that Ang II down-regulated the expression of SM22α and α-SMA and up-regulated the expression of OPN, which were consistent with the results of previous studies. However, BS reversed the effect of Ang II, indicating that BS could inhibit the phenotype switch of VSMCs induced by Ang II.

Phenotype switch of VSMCs is associated with cell migration, which has been reported that 6'-sialyllactose inhibits Ang II-induced VSMC migration by inhibiting ERK1/2/P90Rsk-mediated Akt and NF-κB signaling pathways to prevent atherosclerosis [46]. After phenotype switch, the skeleton of VSMCs was changed including the extension of the pseudopod, the majority of the skeleton F-actin gathering into filamentous microstructures, and the cell morphology changing with no longer spindle [47]. Moreover, cell secretion and the expression of Collagen I are promoted [48]. The results of this study found that Ang II induced VSMCs migration and skeletal remodeling, increased cell secretion, while BS inhibited the effects of Ang II.

The network pharmacology was employed in this study to further investigate the mechanism of BS restrains the phenotype switch of VSMCs. GO enrichment analysis and construction of KEGG signaling pathways revealed that pathways that involved in calcium, toxoplasmosis, and cAMP signaling pathways could be regulated by BS [49, 50]. The cAMP signaling pathway was chosen as the target pathway in this study based on previous relevant research [24, 25]. The molecular docking of BS with cAMP, PKA, and CREB, the three important proteins in the cAMP pathway, demonstrated a good affinity. The level of intracellular cAMP increases after stimulating by external factors and then phosphorylates PKA, which reacts with CREB [25]. Increased cAMP levels in myocardial tissue can activate PKA and exert a protective effect on cardiomyocytes through Ca^{2+} channels [51]. Overexpression of MAP kinase-interacting serine/threonine-protein kinase 2 (MNK2) also inhibits cardiomyocyte apoptosis and cardiac function damage in mice by activating the cAMP/PKA/CREB signaling pathway [52]. The results of this study proved that BS could regulate the cAMP/PKA/CREB signaling pathway. By applying PKA inhibitor, H-89, the results proved that BS could inhibit the phenotype switch of VSMCs and the accompanying excessive proliferation, migration, skeletal remodeling, and cell secretion by activating the cAMP/PKA/CREB signaling pathway.

Conclusion

This study confirmed that BS inhibited the phenotype switch of VSMCs *via* the cAMP/PKA/CREB signaling pathway and excessive cell proliferation, migration, secretion, and skeletal remodeling. The results suggested BS as a basis for further applications and clinical trials and a potential drug for the treatment of cardiovascular diseases. However, this study only verified the relationship between BS and the phenotype switch of VSMCs *in vitro*. Further *in vivo* studies are needed.

Acknowledgements

This study was supported by the National Natural Science Foundation of China (Grant No. 81503282) and Science and Technology Project of Guangdong Province (Grant No. 2014A020212309).

References

1. Mehta PK, Griendling KK. 2007. Angiotensin II cell signaling: physiological and pathological effects in the cardiovascular system. Am J Physiol Cell Physiol. 292(1):C82-C97.
2. Bennett MR, Sinha S, Owens GK. 2016. Vascular smooth muscle cells in atherosclerosis. Circ Res. 118(4):692-702.
3. Lin Y, Zhu W, Chen X. 2020. The involving progress of MSCs based therapy in atherosclerosis. Stem Cell Res Ther. 11(1):216.
4. Yu X, Li Z. 2014. MicroRNAs regulate vascular smooth muscle cell functions in atherosclerosis. Int J Mol Med. 34(4):923-933.
5. Göran KH. 2005. Inflammation, atherosclerosis, and coronary artery disease. New Engl J Med. 352(16):1685-1695.
6. Boucher P, Matz RL, Terrand J. 2020. Atherosclerosis: Gone with the Wnt? Atherosclerosis. 301:15-22.
7. Babu S, Jayaraman S. 2020. An update on beta-sitosterol: A potential herbal nutraceutical for diabetic management. Biomed Pharmacother. 131:110702.
8. Adebiyi OE, Olayemi FO, Olopade JO, Tan NH. 2019. Betaeta-sitosterol enhances motor coordination, attenuates memory loss and demyelination in a vanadium-induced model of experimental neurotoxicity. Pathophysiology. 26(1):21-29.
9. Pierre Luhata L, Usuki T. 2021. Antibacterial activity of beta-sitosterol isolated from the leaves of *Odontonema strictum* (*Acanthaceae*). Bioorg Med Chem Lett. 48:128248.
10. Rogelio PP, Gabriela FM, Celia RL, Brígida HL, Isabel CH, Osiris MS, *et al*. 2017. Evaluation of the anti-inflammatory capacity of beta-sitosterol in rodent assays. Afr J Tradit Complement Altern Med. 14(1):123-130.
11. Yuan LL, Zhang F, Jia S, Xie JH, Shen MY. 2020. Differences between phytosterols with different structures in regulating cholesterol synthesis, transport and metabolism in Caco-2 cells. J Funct Foods. 65(6):103715.
12. Yin YX, Liu XF, Liu JP, Cai EB, Zhu HY, Li HJ, *et al*. 2018. Beta-sitosterol and its derivatives repress lipopolysaccharide/D-galactosamine-induced acute hepatic injury by inhibiting the oxidation and inflammation in mice. Bioorganic Med Chem Lett. 28(9):1525-1533.
13. Chai JW, Lim SL, Kanthimathi MS, Kuppusamy U. 2011. Gene regulation in beta-sitosterol-mediated stimulation of adipogenesis, glucose uptake, and lipid mobilization in rat primary adipocytes. Genes Nutr. 6(2):181-188.
14. Chien M, Lee T, Liang Y, Lee WS. 2010. β-Sitosterol inhibits cell cycle progression of rat aortic smooth muscle cells through increases of p21cip1 protein. J Agric Food Chem. 58(18):10064-10069.
15. Qin Y, Mao W, Pan L, Sun Y, Fan F, Zhao Y, *et al*. 2019. Inhibitory effect of recombinant human CXCL8(3-72)K11R/G31P on atherosclerotic plaques in a mouse model of atherosclerosis. Immunopharmacol Immunotoxicol. 41(3):446-454.
16. Zhang J, Zhao WR, Shi WT, Tan JJ, Zhang KY, Tang JY, *et al*. 2022. *Tribulus terrestris* L. extract ameliorates atherosclerosis by inhibition of vascular smooth muscle cell proliferation in ApoE-/- mice and A7r5 cells *via* suppression of Akt/MEK/ERK signaling. J Ethnopharmacol. 297:115547.
17. Shang L, Wang Y, Li J, Zhou F, Xiao K, Liu Y, *et al*. 2023. Mechanism of Sijunzi Decoction in the treatment of colorectal cancer based on network pharmacology and experimental validation. J Ethnopharmacol. 302(Pt A):115876.
18. Luo Z, Zeng A, Chen Y, He S, He S, Jin X, *et al*. 2021. Ligustilide inhibited Angiotensin II induced A7r5 cell autophagy via Akt/mTOR signaling pathway. Eur J Pharmacol. 905:174184.
19. Chen X, Zhu X, Shen X, Liu Y, Fu W, Wang B. 2023. IGF2BP3 aggravates lung adenocarcinoma progression by modulation of PI3K/AKT signaling pathway. Immunopharmacol Immunotoxicol. 45(3):370-377.
20. Liu Z, Xiang H, Deng Q, Fu W, Li Y, Yu Z, *et al*. 2023. Baicalin and baicalein attenuate hyperuricemic nephropathy via inhibiting PI3K/AKT/NF-κB signalling pathway. Nephrology (Carlton). 28(6):315-327.
21. Hao R, Zhang L, Si Y, Zhang P, Wang Y, Li B, *et al*. 2023. A novel feedback regulated loop of circRRM2-IGF2BP1-MYC promotes breast cancer metastasis. Cancer Cell Int. 23(1):54.
22. Hu L, Liu Y, Dong P, Ye P. 2023. Protective effect of wuzibushen recipe on follicular development via regulating androgen receptor in polycystic ovary syndrome model rats. Gynecol Endocrinol. 39(1):2190808.
23. Wang W, Zhang N. 2023. Oridonin inhibits Hela cell proliferation *via* downregulation of glutathione metabolism: a new insight from metabolomics. J Pharm Pharmacol. 75(6):837-845.
24. Xing D, Bonanno JA. 2009. Effect of cAMP on TGFbeta1-induced corneal keratocyte-myofibroblast transformation. Invest Ophthalmol Vis Sci. 50(2):626-633.
25. Zhu Q, Ni XQ, Lu WW, Zhang JS, Ren JL, Wu D, *et al*. 2017. Intermedin reduces neointima formation by regulating vascular smooth muscle cell phenotype *via* cAMP/PKA pathway. Atherosclerosis. 266:212-222.
26. Davis-Dusenbery BN, Wu C, Hata A. 2011. Micromanaging vascular smooth muscle cell differentiation and phenotypic modulation. Arterioscler Thromb Vasc Biol. 31(11):2370-2377.
27. Durham AL, Speer MY, Scatena M, Giachelli CM, Shanahan CM. 2018. Role of smooth muscle cells in vascular calcification: implications in atherosclerosis and arterial stiffness. Cardiovasc Res. 114(4):590-600.
28. Frismantiene A, Philippova M, Erne P, Resink TJ. 2018. Smooth muscle cell-driven vascular diseases and molecular mechanisms of VSMC plasticity. Cell Signal. 52:48-64.
29. Shin MY, Kwun IS. 2013. Phosphate-induced rat vascular smooth muscle cell calcification and the implication of zinc deficiency in a7r5 cell viability. Prev Nutr Food Sci. 18(2):92-97.
30. Jiang H, Guo Z, Zeng K, Tang H, Tan H, Min R. *et al*. 2023. IL-1β knockdown inhibits cigarette smoke extract-induced inflammation and apoptosis in vascular smooth muscle cells. PloS One. 18(2):e0277719.
31. Chen C, Wu Y, Chan K, Ho H, Wang C, Hsu L. 2022. Mulberry polyphenols ameliorate atherogenic migration and proliferation by degradation of K-Ras and downregulation of its signals in vascular smooth muscle cell. Int J Medical Sci. 19(10):1557-1566.
32. Trott DW, Thabet SR, Kirabo A, Saleh MA, Norlander AE, Wu J, *et al*. 2014. Oligoclonal CD8+ T cells play a critical role in the development of hypertension. Hypertension. 64(5):1108-1115.

33. Li T, Jing J, Sun L, Gong Y, Yang J, Ma C, *et al*. 2023. The SNP rs4591246 in pri-miR-1-3p is associated with abdominal aortic aneurysm risk by regulating cell phenotypic transformation via the miR-1-3p/TLR4 axis. Int Immunopharmacol. 118:110016.
34. Jadli A, Ballasy N, Gomes K, Mackay CDA, Meechem M, Wijesuriya TM, *et al*. 2022. Attenuation of smooth muscle cell phenotypic switching by angiotensin 1-7 protects against thoracic aortic aneurysm. Int J Mol Sci. 23(24):15566.
35. Wang J, Tian X, Yan C, Wu H, Bu Y, Li J, *et al*. 2023. TCF7L1 accelerates smooth muscle cell phenotypic switching and aggravates abdominal aortic aneurysms. JACC: Basic to Translational Science. 8(2):155-170.
36. Guo J, Qiu J, Jia M, Li Q, Wei X, Li L, *et al*. 2023. BACH1 deficiency prevents neointima formation and maintains the differentiated phenotype of vascular smooth muscle cells by regulating chromatin accessibility. Nucleic Acids Res. 51(9):4284-4301.
37. Rong Z, Li F, Zhang R, Niu S, Di X, Ni L, *et al*. 2023. Ant-neointimal formation effects of SLC6A6 in preventing vascular smooth muscle cell proliferation and migration *via* Wnt/β-catenin signaling. Int J Mol Sci. 24(3):3018.
38. Liu Y, Wang X, Wang G, Yang YS, Yuan Y, Ouyang L. 2019. The past, present and future of potential small-molecule drugs targeting p53-MDM2/MDMX for cancer therapy. Eur J Med Chem. 176:92-104.
39. Pan M, Kelman LM, Kelman Z. 2011. The archaeal PCNA proteins. Biochem Soc Trans. 39(1):20-24.
40. Zhao XS, Zheng B, Wen Y, Sun Y, Wen JK, Zhang XH, *et al*. 2019. Salvianolic acid B inhibits Ang II-induced VSMC proliferation *in vitro* and intimal hyperplasia *in vivo* by downregulating miR-146a expression. Phytomedicine. 58:152754.
41. Kim MH, Ham O, Lee SY, Choi E, Lee CY, Park JH, *et al*. 2014. MicroRNA-365 inhibits the proliferation of vascular smooth muscle cells by targeting cyclin D1. J Cell Biochem. 115(10):1752-1761.
42. Wang SC. 2014. PCNA: a silent housekeeper or a potential therapeutic target? Trends Pharmacol Sci. 35(4):178-186.
43. Zhao LL, Zhang F, Chen P, Xie XL, Dou YQ, Lin YL, *et al*. 2017. Insulin-independent GLUT4 translocation in proliferative vascular smooth muscle cells involves SM22alpha. J Mol Med (Berl). 95(2):181-192.
44. Xu D, Gu JT, Yi B, Chen L, Wang GS, Qian GS, *et al*. 2015. Requirement of miR-9-dependent regulation of Myocd in PASMCs phenotypic modulation and proliferation induced by hepatopulmonary syndrome rat serum. J Cell Mol Med. 19(10):2453-2461.
45. Wu M, Liu W, Huang H, Chen Z, Chen Y, Zhong Y, *et al*. 2022. PVT1/miR-145-5p/HK2 modulates vascular smooth muscle cells phenotype switch via glycolysis: The new perspective on the spiral artery remodeling. Placenta. 130:25-33.
46. Nguyen T, Jin Y, Kim L, Heo KS. 2022. Inhibitory effects of 6'-sialyllactose on angiotensin II-induced proliferation, migration, and osteogenic switching in vascular smooth muscle cells. Arch Pharm Res. 45(9):658-670.
47. Russo E, Bertolotto M, Zanetti V, Picciotto D, Esposito P, Carbone F, *et al*. 2023. Role of uric acid in vascular remodeling: Cytoskeleton changes and migration in VSMCs. Int J Mol Med. 24(3):2960.
48. Marulanda J, Alqarni S, Murshed M. 2014. Mechanisms of vascular calcification and associated diseases. Curr Pharm Design. 20(37):5801-5810.
49. Parker T, Wang KW, Manning D, Dart C. 2019. Soluble adenylyl cyclase links Ca(2+) entry to Ca(2+)/cAMP-response element binding protein (CREB) activation in vascular smooth muscle. Sci Rep. 9(1):7317.
50. Liu D, Huang Y, Bu D, Liu AD, Holmberg L, Jia Y, *et al*. 2014. Sulfur dioxide inhibits vascular smooth muscle cell proliferation *via* suppressing the Erk/MAP kinase pathway mediated by cAMP/PKA signaling. Cell Death Dis. 5(5):e1251.
51. Sadek MS, Cachorro E, El-Armouche A, Kammerer S. 2020. Therapeutic implications for PDE2 and cGMP/cAMP mediated crosstalk in cardiovascular diseases. Int J Mol Sci. 21(20):7462.
52. Chen T, Wang Y, Hao Z, Li J. 2021. Parathyroid hormone and its related peptides in bone metabolism. Biochem Pharmacol. 192:114669.